Eur Biophys J (2005) 34: 383–388
DOI 10.1007/s00249-005-0464-1

ARTICLE

Jason Dang · Robert P. Metzger
Robert T. C. Brownlee · Chai Ann Ng
Mikael Bergdahl · Frances Separovic

The conformational flexibility of the antibiotic virginiamycin M_1

Received: 13 November 2004 / Revised: 23 December 2004 / Accepted: 5 January 2005 / Published online: 15 April 2005

Abstract The antibiotic virginiamycin is a combination of two molecules, virginiamycin M_1 (VM1) and virginiamycin S_1 (VS1) or analogues, which function synergistically by binding to bacterial ribosomes and inhibiting bacterial protein synthesis. Both VM1 and VS1 dissolve poorly in water and are soluble in more hydrophobic solvents. We have recently reported that the 3D conformation of VM1 in $CDCl_3$ solution (*Aust. J. Chem.* 57:415, 2004; *Org. Biomol. Chem.* 2:2919, 2004) differs markedly from the conformation bound to a VM1 binding enzyme (Sugantino and Roderick in *Biochemistry* 41:2209, 2002) and to 50S ribosomes (Hansen et al. in *J. Mol. Biol.* 330:1061, 2003) as found by X-ray crystallographic studies. We now report the results of further NMR studies and subsequent molecular modeling of VM1 dissolved in CD_3CN/H_2O and compare the structure with that in CD_3OD and $CDCl_3$. The conformations of VM1 in CD_3CN/H_2O, CD_3OD and $CDCl_3$ differ substantially from one another and from the bound form, with the aqueous form most like the bound structure. We propose that the flexibility of the VM1 molecule in response to environmental conditions contributes to its effectiveness as an antibiotic.

J. Dang · R. T. C. Brownlee · C. A. Ng
Department of Chemistry,
La Trobe University,
Melbourne, VIC, 3086, Australia

R. P. Metzger · M. Bergdahl
Department of Chemistry and Biochemistry,
San Diego State University,
San Diego,
CA 92182-1030, USA

F. Separovic (✉)
School of Chemistry,
University of Melbourne,
Melbourne, VIC,
3010, Australia
E-mail: fs@unimelb.edu.au
Fax: +61-3-9347-5180

Keywords Virginiamycin M_1 · Streptogramin acetyltransferase · Antibiotics · NMR · Molecular structure

Introduction

The streptogramin antibiotics, produced by several species of *Streptomyces*, consist of two components, the macrolactone virginiamycin M_1 (VM1) shown in Fig. 1 and a species-dependent hexadepepsipeptide B component, virginiamycin S_1 (VS1). VM1 and VS1 kill susceptible bacterial strains by inhibiting their protein synthesis (Crooy and De Neys 1972; Paris et al. 1990; Bonfiglio and Furneri 2003). The two components bind synergistically to specific sites on the 23S rRNA of the 50S ribosome, thereby inducing a ribosomal conformational change that strongly interferes with its peptidyl transferase activity (Paris et al. 1990; Bonfiglio and Furneri 2003; Porse and Garrett 1999; Hansen et al. 2003). A recent X-ray crystallographic study clearly shows the conformation of VM1 bound to the 50S ribosome but the location and conformation of the bound B component, VS1, is not well resolved (Hansen et al. 2003). Earlier X-ray crystallographic studies of VM1 bound to the active site of a streptogramin acetyltransferase (Sugantino and Roderick 2002), an enzyme found in some strains of resistant bacteria, showed a conformation essentially identical to that of VM1 bound to the 50S ribosome.

Owing to solubility characteristics, NMR studies of the VM1 conformation in solution have been done in $CDCl_3$ (Kingston et al. 1966; Bycroft 1977; Le Fevre et al. 1983; Surcouf et al. 1990; Dang et al. 2004a), dimethyl sulfoxide (DMSO) and methanol solutions (Dang et al. 2004b). Recently, we reported that the conformations of VM1 in $CDCl_3$, DMSO and CD_3OD, determined by high-resolution NMR experiments (Dang et al. 2004a, 2004b), differ significantly from that of the X-ray crystal structure of VM1 bound to the 50S

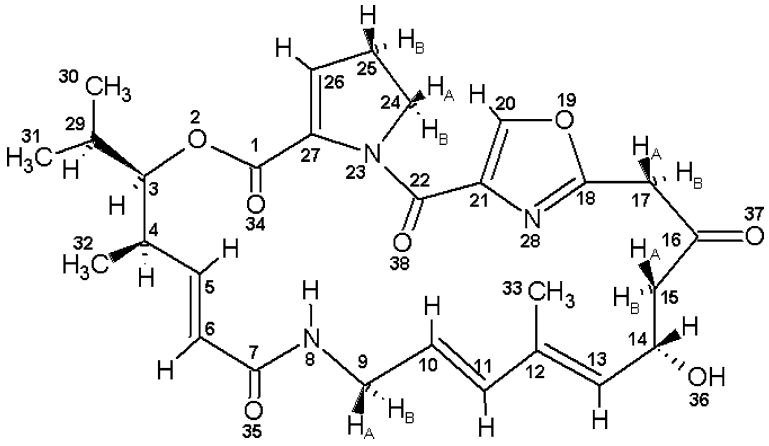

Fig. 1 The chemical structure and numbering of virginiamycin M_1 (*VM1*)

ribosome and to the active site of a streptogramin acetyltransferase enzyme, Vat(D). This implies that the binding process to these entities causes a major change in VM1 conformation.

There are several reasons to determine the conformation of VM1 in aqueous solution or less hydrophobic solvents, including (1) antibiotic synthesis and drug design purposes, (2) the conformation may approximate the VM1 structure in the more hydrophilic environments within the cell, and (3) to understand better changes in conformation as VM1 moves from the free to the bound state in ribosomes and enzymes. Accordingly we now present results of high-resolution NMR studies which verify that the VM1 conformation in aqueous solutions, CD_3CN/H_2O, differs from that in $CDCl_3$, DMSO and CD_3OD and from that of the bound forms (Hansen et al. 2003; Sugantino and Broderick 2002).

Experimental

CD_3CN was obtained from Aldrich (Milwaukee, USA). VM1 was obtained by modification of the procedure of Sharma et al. (1988) as described in Dang et al. (2004b). The recrystallized VM1 was shown to be pure by thin-layer chromatography and 1D ^{1}H NMR.

Owing to the limited solubility of VM1 in water, CD_3CN/H_2O was used to acquire the NMR data: 3.5 mg VM1 in 600 μL of a 17:83 (v/v) solution. Chemical shifts were referenced relative to an appropriate solvent peak and tetramethylsilane set to 0.0 ppm. A Bruker (Karlsruhe, Germany) AVANCE DRX 400 MHz NMR spectrometer was used in this study. 1D ^{1}H NMR ,^{13}C NMR and distortionless enhancement by polarization transfer (DEPT), 2D correlation spectroscopy (COSY) and total correlation spectroscopy (TOCSY) (Claridge 1999; Braun et al. 1998; Ernst et al. 1987), and heteronuclear multiple bond correlation (HMBC) and heteronuclear multiple quantum correlation (HMQC) (Claridge 1999; Braun et al. 1998) spectra were acquired and processed using standard protocols (Claridge 1999; Braun et al. 1998; Ernst et al. 1987). The water signal was suppressed using a double Watergate (w5) field gradient pulse sequence (Braun et al. 1998).

The 2D ^{1}H NMR nuclear Overhauser enhancement spectroscopy (NOESY) (Claridge 1999; Braun et al. 1998; Ernst et al. 1987) and rotating frame Overhauser enhancement spectroscopy (ROESY) spectra (Claridge 1999; Braun et al. 1998) were recorded using a 7.5-μs 90° pulse, 2.0-s relaxation delay and 600-ms mixing time with a spectral width of 11 ppm in each dimension, 2,048 complex data points in F2, 400 increments and 16 transients per increment and Fourier transforming to 2,048 and 1,024 in F2 and F1, respectively. The TOCSY spectra were acquired using a 160-ms mixing time. HMBC (with delay corresponding to 8 Hz) and HMQC experiments used spectral conditions similar to the NOESY but with typically a 12-μs π pulse and 220-ppm spectral width in the ^{13}C dimension, 200 increments, 64 transients per increment and Fourier transforming to 2,048 in both dimensions using appropriate sine-bell apodization.

All 2D NMR spectra were processed using the Bruker XWIN-NMR package and analyzed with the XEASY (Bartels et al. 1995) and SPARKY (Goddard and Kneller 2004) software for chemical shift and NOE attributions with the $H15_{AB}$ NOE, corresponding to a distance of 1.79 Å, used to calibrate the NOEs of the nonaromatic protons. Distance constraints from the NOESY and ROESY spectra were classified as strong (1.8–2.7 Å), medium (2.7–3.5 Å), weak (3.5–5.0 Å) and very weak (5.0–6.0 Å) (Clore et al. 1986). Simulated annealing was used to generate structures using the DYANA and CYANA programs (Güntert et al. 1997). Two hundred structures were calculated from an extended structure using a torsion mode and distance constraints derived from NOESY and ROESY experiments, with a total of 44 distance constraints for CD_3CN/H_2O. Twenty structures that satisfied the experimental constraints with violations less than 0.5 Å were selected as the global fold of VM1.

Dynamics and energy calculations were performed using Insight and Discover software (Accelrys, San Diego, USA) using the consistent-valence force field (CVFF) and the steepest descent and conjugate gradients methods. The 20 structures that satisfied all

the distance constraints from DYANA's structural calculations were chosen as the starting conformers for energetic calculations.

The docking studies of VM1 with the enzyme Vat(D) and 50S ribosome were performed on an SGI (Mountain View, USA) Octane computer using the Accelrys program. The VM1 structure in the appropriate solution was superimposed onto the VM1 in the active site of the X-ray crystal structure and the X-ray VM1 structure was then removed. Conjugated gradient minimization was then performed on the VM1 structure now present in the active site.

Results and discussion

The assignments of the ^{1}H and ^{13}C NMR spectra of VM1 in CD_3CN/H_2O determined using 2D NMR and DEPT experiments (Claridge 1999; Braun et al. 1998) are shown in Table 1. All assignments were made using a combination of DEPT, HMQC, HMBC, COSY and TOCSY spectra (Claridge 1999; Braun et al. 1998; Ernst et al. 1987) to eliminate ambiguities.

Figure 2 depicts the VM1 conformations derived from distance constraints from NOESY and ROESY connectivities. Owing to the low molecular weight of VM1, ROESY experiments resulted in more long-range proton connectivities than NOESY experiments (Claridge 1999; Braun et al. 1998). For the solution structure of VM1 in CD_3CN/H_2O, the average of the global backbone root-mean square deviations came to 0.36 ± 0.23 Å and gave calculated conformational energies (Table 2) comparable to those found for VM1 in other solvents and the X-ray structure (Dang et al. 2004b). Note that the oxazole ring and the nitrogen 8/H8 vector (Figs. 1, 2c) in the aqueous solution conformation for VM1 appear to be rotated approximately 100° for the oxazole ring and of order 20° for N8/H8 compared with those of the bound form (Fig. 2d).

The conformation of VM1 in CD_3CN/H_2O solution appears to differ markedly from that of VM1 bound to the 50S ribosome and the active site of Vat(D), and also from those found in CD_3OD, DMSO and $CDCl_3$ solvents (Fig. 3). The VM1 conformations determined from NMR experiments in $CDCl_3$, DMSO and CD_3OD are more compact than that in CD_3CN/H_2O. Interestingly, however, the latter shows somewhat greater similarity to the structure of VM1 bound to the active site of Vat(D) or to the 50S ribosome, in that the VM1 structure is a more extended or flatter conformation.

In Fig. 4, our solution conformations are compared with the conformation in the X-ray structure of VM1 bound to the active site of Vat(D) (PDB ID 1KK6) (Sugantino and Roderick 2002). The structure of the bound form of VM1 in the enzyme (Fig. 4) and the 50S ribosome (PDB ID 1N8R) (Hansen et al. 2003) (Fig. 5) are almost identical.

The X-ray structure of Hansen et al. (2003), a milestone in structural biology, shows clearly the location and conformation of VM1 in the ribosome (Fig. 5). VM1 bound to either ribosome or enzyme is flattened and spread out, almost to the maximum extent

Table 1 ^{1}H and ^{13}C chemical shifts of virginiamycin M1 (*VM1*) in CD_3CN/H_2O at 30°C

VM1 atom type	H1 δ (ppm)	C13 δ (ppm)	J (Hz)
H30A	0.81	18.46	$^{3}J_{30,29} = 6.45$
H30B	0.81	18.46	
H30C	0.81	18.46	
H31A	0.87	17.72	$^{3}J_{30,29} = 6.98$
H31B	0.87	17.72	
H31C	0.87	17.72	
H32A	1.02	10.44	$^{3}J_{32,4} = 7.25$
H32B	1.02	10.44	
H32C	1.02	10.44	
H29	1.91	28.97	
H4	2.74[a]	36.54	
H3	4.76[a]	81.28	
H6	5.96	123.01	$^{3}J_{6,5} = 18.27$
H5	6.59	145.78	$^{3}J_{5,6} = 16.92$; $^{3}J_{5,4} = 6.18$
C7	NA	167.50	
H33A	1.54	11.68	
H33B	1.54	11.68	
H33C	1.54	11.68	
H15A	2.76[a]	48.36	
H15B	2.99	48.36	
H9A	3.72	40.38	
H9B	3.92	40.38	
H14	4.76[a]	64.29	
H13	5.14	130.53	$^{3}J_{13,14} = 9.4$
H10	5.58	125.22	$^{3}J_{10,11} = 16.4$
H11	5.85	134.54	$^{3}J_{11,10} = 17.46$
H8	7.73	–	
C12	NA	134.45	
C16	NA	204.09	
H17A	3.82	43.24	$^{2}J_{17A,B} = 16.66$
H17B	4.00	43.24	$^{2}J_{17B,A} = 15.04$
H20	8.13	144.26	
C21	NA	135.10	
C18	NA	157.61	
C22	NA	160.89	
H25A	2.65	29.41	
H25B	2.65	29.41	
H24A	3.97	51.15	
H24B	4.06	51.15	
H26	6.40	128.87	$^{3}J_{26,25A} = 2.96$; $^{3}J_{26,25B} = 2.96$
C27	NA	136.19	
C1	NA	161.26	

The ^{1}H chemical shifts at 400 MHz and the ^{13}C chemical shifts at 100 MHz are given.
[a]Overlapping peaks

Table 2 Analysis of the 20 energy-minimized structures used to represent the solution structure of VM1 in CD_3CN/H_2O

Conformational energy in CD_3CN/H_2O	
E_{total}	40.12 ± 1.56 kcal/mol
E_{NOE}	3.80 ± 1.26 kcal/mol
E_{bond}	8.31 ± 0.42 kcal/mol
E_{ϕ}	25.28 ± 2.12 kcal/mol
$E_{repulsion}$	131.29 ± 1.61 kcal/mol
$E_{dispersion}$	-117.50 ± 1.14 kcal/mol
Average of the global backbone root-mean square deviations	0.36 ± 0.23 Å

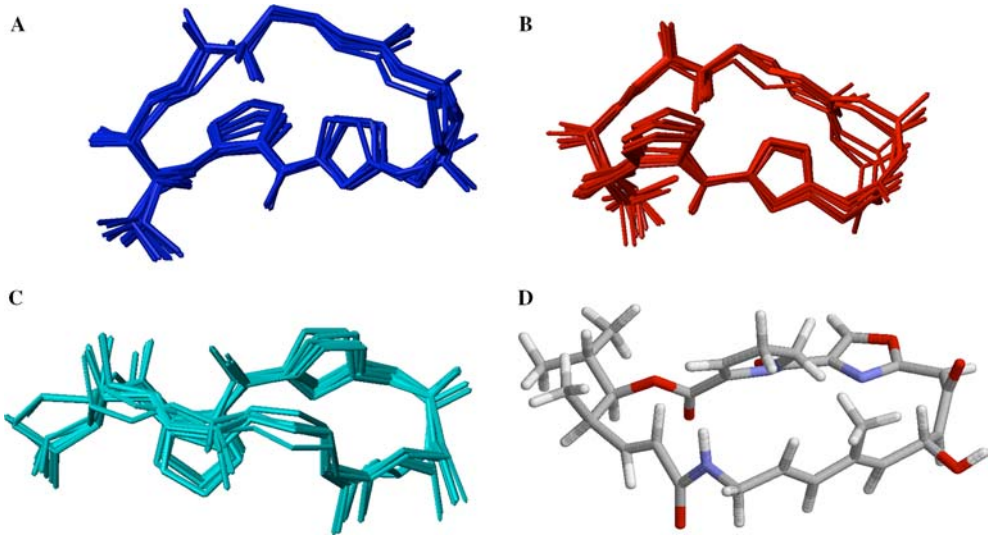

Fig. 2 The conformations of VM1 **a** in $CDCl_3$ (Dang et al. 2004a), **b** in CD_3OD (Dang et al. 2004b) and **c** in CD_3CN/H_2O, and **d** a representation of VM1 bound to the 50S ribosome (Hansen et al. 2003). Note that the proline ring is at the back of each structure

(Fig. 3), undoubtedly aided by hydrophobic and polar interactions between molecular groups and the binding sites. Yet our data suggest that the aqueous environment itself, probably as a result of polar interactions between the solvent and hydrophilic groups in VM1, causes the antibiotic to assume a flattened structure, somewhat similar to that of the bound form. Nevertheless, there is no doubt as to the importance of hydrophobic interactions in the binding of the VM1 to its ribosomal and Vat(D) sites. The VM1 oxazole enters a ribosomal hydrophobic pocket, causing a rotation of a ribosomal adenosine component (Hansen et al. 2003). This allows hydrophobic interactions between the base and the conjugated NH8, and a hydrophilic interaction of the adenosine 2′E OH group with the carbonyl O35 of VM1 and there is an additional interaction between the hydroxyl group (O36/H36) on VM1 and another ribosomal adenosine (Hansen et al. 2003).

Sugantino and Roderick (2002) suggest that the Vat(D) active site binds VM1 by hydrophobic interaction, together with hydrophilic interactions of an aspartate with O37 and an asparagine with O35. The interaction of a tyrosine and a serine with the hydroxyl group (O36/H36) is also apparent (Fig. 4). It may well be that the key to conformational change of VM1 from solution to bound form lies at the conjugated N8/H8, and the hydroxyl group (O36/H36). Our docked structure (Fig. 4) shows that the oxazole ring and N8/H8 in our proposed conformations for VM1 in CD_3CN/H_2O (and also CD_3OD and $CDCl_3$) appear to be rotated differently compared with the conformation of the bound form, as discussed earlier and in the legend to Fig. 4. The solution conformations of VM1 show the observed ROESY connectivities between H20 and H8, H9A/H9B and H11, supporting the change in orientation of the ring. The mechanism of the binding process itself most probably causes a

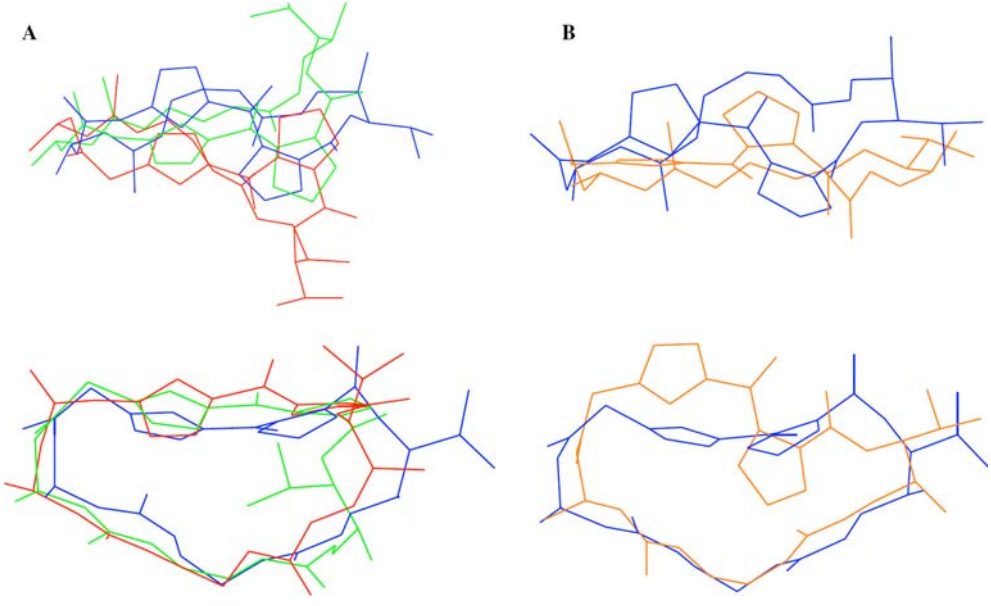

Fig. 3 Two views showing the superposition of the average structures of VM1. **a** In $CDCl_3$ (*red*), in CD_3OD (*green*) and in CD_3CN/H_2O (*blue*). **b** A comparison of the CD_3CN/H_2O (*blue*) NMR structure with the X-ray structure of VM1 bound to a streptogramin acetyltransferase enzyme, *Vat(D)*, or the 50S ribosome. The images were produced using VMD (Humphrey et al. 1996) software

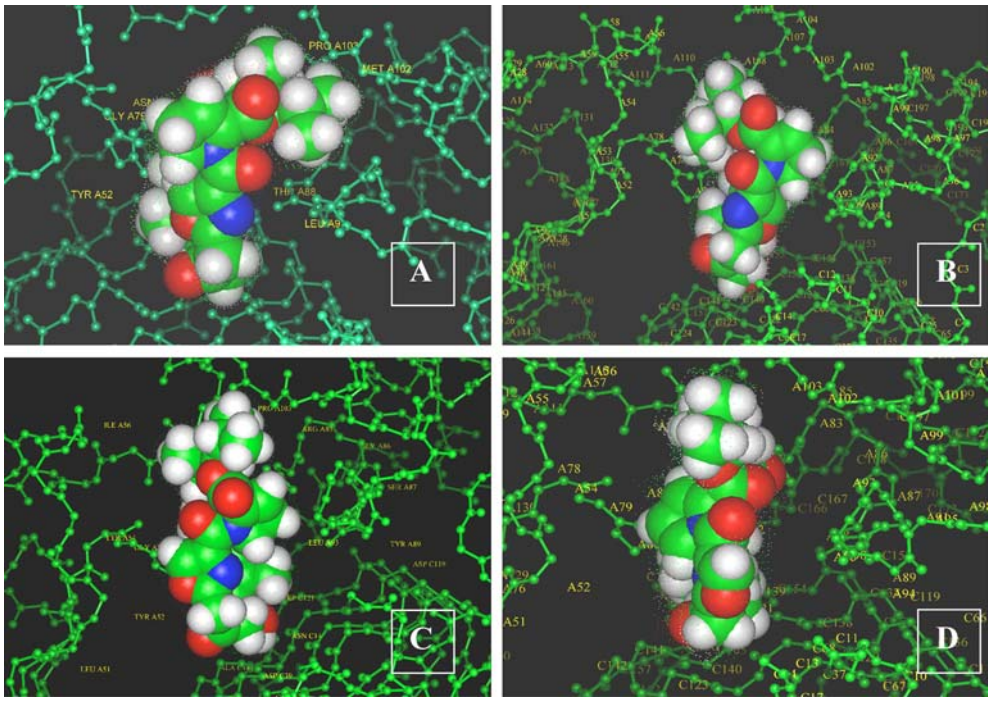

Fig. 4 The energy-minimized structure of VM1 obtained from NMR data in **a** $CDCl_3$, **b** CD_3OD and **c** CD_3CN/H_2O with VM1 docked into Vat(D). **d** X-ray structure of VM1 in Vat(D) (PDB ID 1KHR). Only atoms of Vat(D) that surround VM1 within 15 Å are displayed. Although the structure of VM1 in CD_3CN/H_2O is closest to the X-ray [Vat(D)-bound] structure, the oxazole ring is rotated by approximately 100° and the N8/H8 bond by roughly 20°, when compared with one another

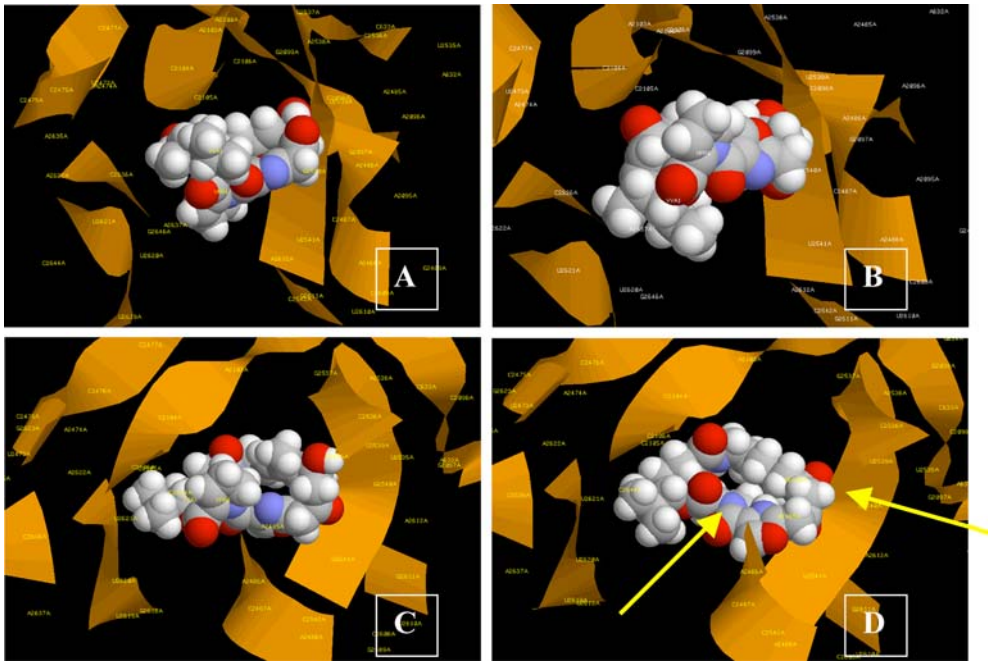

Fig. 5 The energy-minimized structure of VM1 obtained from NMR data in **a** $CDCl_3$, **b** CD_3OD and **c** CD_3CN/H_2O with VM1 inserted into the 50S ribosome binding sites. **d** The crystal structure of the 50S ribosome with bound VM1 (PDB ID 1N8R). Only atoms of 50S ribosome that surround VM1 within 15 Å are displayed (backbone representation). *Arrows* indicate the oxazole and N8/H8 groups

conformational change as well as inherent solvent differences. We propose that the flexibility of the VM1 molecule in response to environmental conditions contributes to its effectiveness as an antibiotic.

Acknowledgements J.D. and C.A.N. gratefully acknowledge receipt of financial support from La Trobe University. We thank LeRoy Lafferty (SDSU) for obtaining the 500 MHz NMR spectra.

References

Bartels C, Xia TH, Billeter M, Güntert P, Wüthrich K (1995) The program XEASY for computer supported NMR spectral analysis of biological macromolecules. J Biomol NMR 5:1–10

Bonfiglio G, Furneri PM (2003) Patents on streptogramin antibiotics. Expert Opin Ther Patents 13:651–659

Braun S, Kalinowski H-O, Berger S (1998) 150 and more basic NMR experiments. Wiley, Weinheim

Bycroft BW (1977) Configurational and conformational studies on the group A peptide antibiotics of the mikamysin (streptogramin, virginiamycin) family. J Chem Soc Perkin I p 2464–2470

Claridge TDW (1999) High-resolution NMR techniques in organic chemistry. Pergamon Press, New York

Clore GM, Nilges M, Sukurama DK, Brunger AT, Karplus M, Gronenborn AM (1986) The three-dimensional structure of A1-purothionin in solution: combined use of nuclear magnetic resonance, distance geometry and restrained molecular dynamics. EMBO J 5:2729–2735

Crooy P, De Neys R (1972) Virginiamycin: nomenclature. J Antibiot 25:371–372

Dang J, Bergdahl BM, Separovic F, Brownlee RTC, Metzger RP (2004a) Virginiamycin M1 conformation in solution differs from the form bound to the 50S ribosome and to streptogramin acetyltransferase. Aust J Chem 57:415–418

Dang J, Separovic F, Bergdahl M, Brownlee RTC, Metzger RP (2004b) Solvent affects the conformation of virginiamycin M1 (pristinamycin IIA, streptogramin A). Org Biomol Chem 2:2919–2924

Ernst RR, Bodenhausen G, Wokaun A (1987) Principles of nuclear magnetic resonance in one and two dimensions. Clarendon Press, Oxford

Goddard TD, Kneller DG (2004) SPARKY 3. University of California, San Francisco

Güntert P, Mumenthaler C, Wüthrich K (1997) Torsion angle dynamics for NMR structure calculations with the new program DYANA. J Mol Biol 273:283–298

Hansen JL, Moore PB, Steitz TA (2003) Structures of five antibiotics bound at the peptidyl transferase center of the large ribosomal subunit. J Mol Biol 330:1061–1075

Humphrey W, Dalke A, Schulten K (1996) VMD—Visual Molecular Dynamics. J Molec Graphics 14:33–38

Kingston DGI, Todd L, Williams DH (1966) Antibiotics of the ostreogrycin complex. Part III. The structure of ostreogrycin A. Evidence based on nuclear magnetic double resonance experiments and high resolution mass spectroscopy. J Chem Soc C 1669–1676

Le Fevre JW, Glass TE, Kolpak MK, Kingston DGI, Chen PN (1983) Biosynthesis of antibiotics of the virginiamycin family. Assignment of the ^{13}C-NMR spectra of virginiamycin M_1 and antibiotic A2315A. J Nat Prod 46:475–480

Paris JM, Barrière JC, Smith C, Bost PE (1990) The chemistry of pristinamycins. In: Lukacs G, Ohno M (eds) Recent progress in the chemical synthesis of antibiotics. Springer, Berlin Heidelberg New York pp 183–248

Porse BT, Garrett RA (1999) Sites of interaction of streptogramin A and B. Antibiotics in the peptidyl transferase loop of 23 S rRNA and the syngergism of their inhibitory mechanisms. J Mol Biol 286:375–387

Sharma NK, Hosten N, Anteunis MJO (1988) Isolation of factor A (virginiamycin M_1) and factor B (mixture of VS1 and VS4) from a commercial feed additive formulation. Bull Soc Chim Belges 97:185–192

Sugantino M, Roderick SL (2002) Crystal structure of Vat(D). An acetyltransferase that inactivates streptogramin group A antibiotics. Biochemistry 41:2209–2216

Surcouf E, Morize I, Frechet D, Vuilhorgne M, Mikou A, Guitet E, Lallemand JY (1990) Molecular dynamics study of prisinamycin IIA from crystal structure to conformation in apolar solvent using NMR data. Stud Phy Theor Chem 71:719–726